

terms (n , k^F , and ψ) adapted to give a maximum in $E(\phi)$ at $\phi = 180^\circ$ are given by eqs 7-9.

Appendix 2

The SHAPES force field is the three-dimensional generalization of the Fourier angular potential expressions. In order to illustrate the SHAPES formulation and its relationship to the AOM we will first consider angular distortions for ammonia according to the AOM.¹⁵ For this discussion the geometric arrangement and angle definitions illustrated in Figure 2 are adopted. Two distortion coordinates, θ (the angle formed by the z axis and the N-H bond vector, or the inversion coordinate) and ϕ (the angle formed by the projections of the N-H bond vectors into the x - y plane), are considered with the simplifying constraints that $\theta_1 = \theta_2 = \theta_3$ and $\phi_{12} = \phi_{23} = \phi_{13}$. According to the p-orbital AOM (i.e. utilizing the 2p orbitals, only, of the nitrogen) the total energy is given by

$$E_{\text{AOM}} = 4e_{\sigma}[(1 + 2 \cos^2 \phi)(\sin^2 \theta) + 2 \sin^2 \phi \sin^2 \theta + 3 \cos^2 \theta] - 4f_{\sigma}[(1 + 2 \cos^2 \phi)^2(\sin^4 \theta) + 4 \sin^4 \theta \sin^4 \phi + 9 \cos^4 \theta] \quad (17a)$$

$$E_{\text{AOM}}^{\text{strain}} = 12f_{\sigma} - 4f_{\sigma}\{[5 + (4 \cos^2 \phi)(2 \cos^2 \phi - 1)][\sin^4 \theta] + 9 \cos^4 \theta\} \quad (17b)$$

These expressions lead to a total of four minima symmetrically disposed about $\phi = 90^\circ$ and $\theta = 90^\circ$. Two of these minima ($\phi = 120^\circ$ and $\theta = 54.7^\circ$ and 125.3°) closely correspond to the experimental structure of NH_3 ($\phi = 120^\circ$ and $\theta \approx 59^\circ$ and 121°) whereas the two minima at $\phi = 60^\circ$ and $\theta = 54.7^\circ$ and 125.3° are not observed. The second set of minimum energy structures occurs because the AOM does not take into account interligand overlaps (1,3-interactions). Note that the ϕ terms of expression 17b are multiplied by $\sin^4 \theta$, reflecting decreasing overlap of the p_x and p_y orbitals of the central nitrogen with the ligands as the ligands are displaced from the x - y plane. These changes give rise

to the weighting formula used in SHAPES (eq 11), where $\sin \theta \approx r_{\text{ML}}/R_{\text{ML}}$.

Acknowledgment. Partial support of this work by the donors of the Petroleum Research Fund, administered by the American Chemical Society, is gratefully acknowledged. We thank the Monsanto Company and Syntex Corp. for additional support. Polygen Corp. supplied us with the source code for the CHARMM program for which we are most thankful. We thank A. K. Rappe for providing us with the computer code for the calculation of partial charges by the charge equilibration method and for many helpful discussions. Finally, we acknowledge P. J. Hay for his assistance in using the MESA computational package and for his encouragement and advice.

Registry No. 8, 75085-37-9; 9, 91514-09-9; 10, 75421-75-9; 11, 70196-22-4; 12, 97860-28-1; 13, 60362-57-4; 14, 70376-39-5; *trans*-Pd(NH_3)₂Cl₂, 13782-33-7; *trans*-Pt(NH_3)₂Cl₂, 14913-33-8; [Rh(PH_3)₄]⁺, 121176-09-8; [PdCl₄]²⁻, 14349-67-8; [Pt(NH_3)₄]²⁺, 16455-68-8; [Pd(NH_3)₄]²⁺, 15974-14-8; [Pd(PMe₃)Cl₃]⁻, 44630-56-0; [Pt(PMe₃)Cl₃]⁻, 44630-63-9; *trans*-¹⁰⁴Pd(PET₃)₂Cl₂, 29303-43-3; *trans*-¹¹⁰Pd(PET₃)₂Cl₂, 130434-99-0; [Pt(C₂H₄)Cl₃]⁻, 12275-00-2; [Pt(C₂D₄)Cl₃]⁻, 69030-45-1; [Rh(C₂H₄)₂Cl]₂, 12081-16-2; *trans*-Rh(PMe₃)₂(CO)Cl, 22710-50-5; *trans*-Pt(PH₃)₂Cl₂, 79389-91-6; *trans*-Pd(PH₃)₂Cl₂, 72360-10-2; [PtCl₄]²⁻, 13965-91-8.

Supplementary Material Available: Tables of the results of normal coordinate analyses of [PtCl₄]²⁻, [PdCl₄]²⁻, [Pt(NH₃)₄]²⁺, [Pd(NH₃)₄]²⁺, *trans*-Pt(NH₃)₂Cl₂, *trans*-Pd(NH₃)₂Cl₂, [Pd(PMe₃)Cl₃]⁻, [Pt(PMe₃)Cl₃]⁻, *trans*-¹⁰⁴Pd(PET₃)₂Cl₂ and *trans*-¹¹⁰Pd(PET₃)₂Cl₂, [Pt(C₂H₄)Cl₃]⁻ and [Pt(C₂D₄)Cl₃]⁻, [Rh(C₂H₄)₂Cl]₂, and *trans*-Rh(PMe₃)₂(CO)Cl, the HF-SCF optimized geometries for *trans*-Pt(NH₃)₂Cl₂, *trans*-Pt(PH₃)₂Cl₂, *trans*-Pd(NH₃)₂Cl₂, *trans*-Pd(PH₃)₂Cl₂, and [Rh(PH₃)₄]⁺, and tabulation of SHAPES calculated and experimental structures for compounds 1-14 (51 pages). Ordering information is given on any current masthead page.

Formation of Self-Assembled Monolayers by Chemisorption of Derivatives of Oligo(ethylene glycol) of Structure HS(CH₂)₁₁(OCH₂CH₂)_mOH on Gold¹

Catherine Pale-Grosdemange, Ethan S. Simon, Kevin L. Prime,[†] and George M. Whitesides*

Contribution from the Department of Chemistry, Harvard University, Cambridge, Massachusetts 02138. Received May 21, 1990

Abstract: This paper describes the preparation of oligo(ethylene glycol)-terminated alkanethiols having structure HS-(CH₂)₁₁(OCH₂CH₂)_mOH ($m = 3-7$) and their use in the formation of self-assembled monolayers (SAMs) on gold. A combination of experimental evidence derived from X-ray photoelectron spectroscopy (XPS), measurement of contact angles, and ellipsometry implies substantial disorder in the oligo(ethylene glycol)-containing segment. The order in the -(CH₂)₁₁- group is not defined by the available evidence. The SAMs are moderately hydrophilic: $\theta_a(\text{H}_2\text{O}) = 34-38^\circ$; $\theta_r(\text{H}_2\text{O}) = 22-25^\circ$. A study of monolayers containing mixtures of HS(CH₂)₁₁CH₃ and HS(CH₂)₁₁(OCH₂CH₂)₆OH suggests that the oligo(ethylene glycol) moieties are effective at preventing underlying methylene groups from influencing wetting by water. A limited study demonstrates that these oligo(ethylene glycol)-containing SAMs resist the adsorption of protein from solution and suggests that SAMs will be a useful model system for studying the adsorption of proteins onto organic surfaces.

Introduction

Oligomers of ethylene glycol are moderately hydrophilic groups: The Hansch π parameter for ethylene glycol is ~ -1.93 .² These oligomers are commonly incorporated as components of materials when increased hydrophilicity is required³ and have proved useful as constituents of biocompatible materials.⁴ The structure of the

oligo(ethylene glycol) units at a solid-water interface is relevant to the molecular level design of materials having desired degrees

(1) The research described in this paper was supported by the National Science Foundation under the Engineering Research Center Initiative to the MIT Biotechnology Process Engineering Center (Cooperative Agreement CDR-88-03014), by the Office of Naval Research and the Defense Advanced Research Projects Agency, and by the NIH (GM39589). The XPS was provided by DARPA through the University Research Initiative and is housed in the Harvard University Materials Research Laboratory, an NSF-funded facility.

[†] NSF Predoctoral Fellow, 1986-1989.

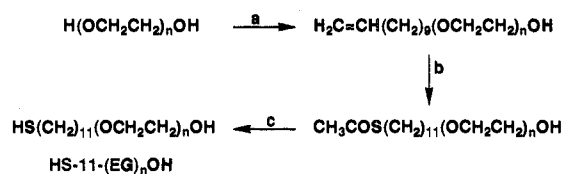
of hydrophilicity and adsorptivity toward biological (and other) molecules.⁵

As part of a program to explore the physical organic chemistry of the interaction of biological molecules with surfaces, we have prepared materials incorporating oligomers of ethylene glycol into self-assembled monolayers (SAMs) of alkanethiolates on gold.^{6,7} The objective of this work was to apply these SAMs—with whatever degree of structural order characterized them—to the study of the solid–water interfacial properties of materials having oligo(ethylene glycol) moieties as constituents. This paper describes the preparation of SAMs by chemisorption of compounds of structure $\text{HS}(\text{CH}_2)_{11}(\text{OCH}_2\text{CH}_2)_m\text{OH}$ ($m = 0, 3-7$) onto gold, the characterization of these SAMs, and preliminary measurements of their adsorptivity toward proteins in solution.

SAMs derived from unfunctionalized alkanethiols $\text{HS}(\text{CH}_2)_n\text{CH}_3$ are easily prepared by reaction of solutions or vapors of these compounds with gold.⁸⁻²⁰ The polymethylene chains in these SAMs are predominantly trans-extended when $n \geq 10$, although the terminal segments of the chains (those at the monolayer–vapor or –liquid interface) contain some gauche bonds: when $n = 10$, the monolayers contain more gauche bonds than when $n = 17$.^{12,15-17} With terminally functionalized alkanethiols $\text{HS}(\text{CH}_2)_n\text{R}$, the size and shape of the R group are important. When R is small, the $(\text{CH}_2)_n$ -containing regions of the SAMs are still predominantly trans-extended.¹⁷ When R is large, we presume that the polymethylene regions of the SAMs contain a greater fraction of gauche bonds; i.e., they are more disordered.²¹

Our choice of the structure $\text{HS}(\text{CH}_2)_{11}(\text{OCH}_2\text{CH}_2)_m\text{OH}$ containing only 11 methylene groups as the basis for this work was a compromise between convenience of preparation and structural order in the SAMs. Monolayers containing the $\text{HS}(\text{CH}_2)_{11}$ - moiety could be expected to have more gauche bonds

Scheme I. Synthesis of ω -Mercapto-oligo(ethylene glycol) Derivatives, $\text{HS}(\text{CH}_2)_{11}(\text{OCH}_2\text{CH}_2)_n\text{OH}$ ($n = 3-7$)^a



^a Key: (a) $\text{CH}_2=\text{CH}(\text{CH}_2)_9\text{Br}$, 50% aqueous NaOH, 100 °C, 24 h (63–87%); (b) CH_3COSH , AIBN, $h\nu$, 4 h (79–88%); (c) 0.1 M HCl in MeOH; Reflux, 4 h; or room temperature, 4–5 days (81–90%).

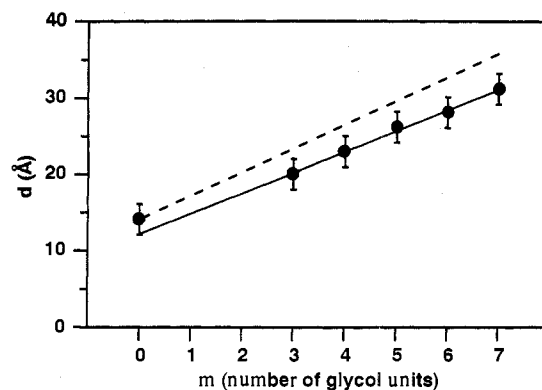


Figure 1. Thicknesses (d , Å) of monolayers of ω -mercapto-oligo(ethylene glycol) derivatives $\text{HS}(\text{CH}_2)_{11}(\text{OCH}_2\text{CH}_2)_m\text{OH}$ ($\text{HS-11-(EG)}_m\text{OH}$) determined by ellipsometry. The dotted line shows the predicted thickness for monolayers of these molecules in fully trans-extended arrays at a cant angle of 30°. The incremental increase in the thickness per $-\text{OCH}_2\text{CH}_2-$ unit is 2.7 Å; that calculated per $-\text{OCH}_2\text{CH}_2-$ unit is 3.1 Å.

(2) Leo, A.; Hansch, C.; Elkins, D. *Chem. Rev.* **1971**, *71*, 525. Other relevant π -parameters are the following: di(ethylene glycol), -1.98 ; tri(ethylene glycol), -2.08 ; tetra(ethylene glycol), -2.18 . For reference, values of π for other functional groups are the following: $-\text{CONH}_2$, -1.71 ; $-\text{CH}_2\text{OH}$, -1.03 ; $-\text{CO}_2\text{CH}_3$, -0.27 ; $-\text{CO}_2\text{H}$, -0.67 ; $-\text{COCH}_3$, -0.71 .

(3) *Kirk-Othmer Encyclopedia of Chemical Technology*; Wiley-Interscience: New York, 1980; Vol. 9, p 432.

(4) For examples, see: Lee, J. H.; Kopecek, J.; Andrade, J. D. *J. Biomed. Mater. Res.* **1989**, *23*, 351. Lee, J. H.; Kopeckova, P.; Kopecek, J.; Andrade, J. D. *Biomaterials*, in press. Jeon, S. I.; Lee, J. H.; Andrade, J. D.; de Gennes, P. G. *J. Colloid Interface Sci.*, in press. Andrade, J. D.; Hlady, V. *Adv. Polym. Sci.* **1986**, *79*, 1. *Hydrogels in Medicine and Pharmacy*; Peppas, N. A., Ed.; CRC: Boca Raton, FL, 1986, 1987; Vols. 1–3. Allmér, K.; Hilborn, J.; Larsson, P. H.; Hult, A. Rånby, B. *J. Polym. Sci.*, in press. Mauzac, M.; Aubert, N.; Josefovicz, M. *Biomaterials* **1982**, *3*, 221. Cho, C. S.; Kim, S. W. *J. Controlled Release* **1988**, *7*, 283. Cohn, D.; Younes, H. *J. Biomed. Mater. Res.* **1988**, *22*, 993.

(5) Hench, L. L. *Biomaterials: An Interfacial Approach*; Academic: New York, 1982.

(6) Whitesides, G. M.; Ferguson, G. S. *Chemtracts: Org. Chem.* **1988**, *1*, 171.

(7) Bain, C. D.; Whitesides, G. M. *Angew. Chem.* **1989**, *101*, 522.

(8) Bain, C. D.; Whitesides, G. M. *Science (Washington D.C.)* **1988**, *240*, 62.

(9) Bain, C. D.; Whitesides, G. M. *J. Am. Chem. Soc.* **1988**, *110*, 6560.

(10) Bain, C. D.; Whitesides, G. M. *J. Am. Chem. Soc.* **1988**, *110*, 5897.

(11) Bain, C. D.; Whitesides, G. M. *J. Am. Chem. Soc.* **1988**, *110*, 3665.

(12) Bain, C. D.; Troughton, E. B.; Tao, Y.-T.; Evall, J.; Whitesides, G. M.; Nuzzo, R. G. *J. Am. Chem. Soc.* **1989**, *111*, 321.

(13) Nuzzo, R. G.; Fusco, F. A.; Allara, D. L. *J. Am. Chem. Soc.* **1987**, *109*, 2358.

(14) Nuzzo, R. G.; Allara, D. L. *J. Am. Chem. Soc.* **1983**, *105*, 4481.

(15) Porter, M. D.; Bright, T. B.; Allara, D. L.; Chidsey, C. E. D. *J. Am. Chem. Soc.* **1987**, *109*, 3559.

(16) Barton, S. W.; Thomas, B. N.; Flom, E. B.; Rice, S. A.; Lin, B.; Peng, J. B.; Ketterson, J. B.; Dutta, P. *J. Chem. Phys.* **1988**, *89*, 2257 and references therein. Bareman, J. P.; Cardini, G.; Klein, M. L. *Phys. Rev. Lett.* **1988**, *60*, 2152 and references therein.

(17) Nuzzo, R. G.; Dubois, L. H.; Allara, D. L. *J. Am. Chem. Soc.* **1990**, *112*, 558.

(18) Sundgren, J.-E.; Bodö, P.; Ivarsson, B.; Lundstroem, I. *J. Colloid Interface Sci.* **1986**, *113*, 530.

(19) Finklea, H. O.; Avery, S.; Lynch, M.; Furtch, T.; *Langmuir* **1987**, *3*, 409.

(20) Diem, T.; Czajka, B.; Weber, B.; Regen, S. L. *J. Am. Chem. Soc.* **1986**, *108*, 6094.

(21) Prime, K. L.; Whitesides, G. M. Unpublished results.

in the polymethylene region than longer chain analogues (e.g., $\text{HS}(\text{CH}_2)_{18}$), but the thiols are more easily synthesized and purified than are these longer chain compounds. The compounds with structures $\text{HS}(\text{CH}_2)_{11}(\text{OCH}_2\text{CH}_2)_m\text{OH}$ are easily manipulated: They are soluble in ethanol and stable in air, and they form monolayers rapidly and reproducibly by chemisorption onto gold. The $\text{HS}(\text{CH}_2)_{11}$ - moiety provides a foundation for stable SAMs, and we expected the oligo(ethylene glycol) derivatives of this group also to be sufficiently stable for our studies.

This work describes the syntheses of oligo(ethylene glycol)-terminated alkanethiols and the characterization of one- and two-component SAMs on gold containing them. We examined these monolayers by X-ray photoelectron spectroscopy (XPS), ellipsometry, polarized infrared external reflectance spectroscopy (PIERS), and measurement of contact angles; our results suggest that the oligo(ethylene glycol) groups in these SAMs are not highly ordered. The thickness of the portions of the films occupied by these groups, furthermore, appeared to be $\sim 15\%$ less than that expected if they occupied an ordered, trans-extended configuration. The thermal and mechanical stabilities of these SAMs were adequate for exploratory studies of protein adsorption: They did not spontaneously desorb from gold in the time and conditions required for our experiments (hours to days, in contact with water at room temperature).²² We describe preliminary results from a study of the adsorption of several representative proteins to these oligo(ethylene glycol)-containing SAMs; further studies of protein adsorption will be described in a subsequent paper.

For simplicity, we use the shorthand notation $\text{HS-11-(EG)}_m\text{OH}$ to refer to $\text{HS}(\text{CH}_2)_{11}(\text{OCH}_2\text{CH}_2)_m\text{OH}$.

Results

Synthesis of Thiols. Thiols incorporating oligo(ethylene glycol) moieties were prepared via a three-step synthesis (Scheme I). The reaction of an 11-haloundec-1-ene with a slight excess of 50% sodium hydroxide and 3–10 equiv of oligo(ethylene glycol) pro-

(22) The desorbed species in these systems is probably RSSR.

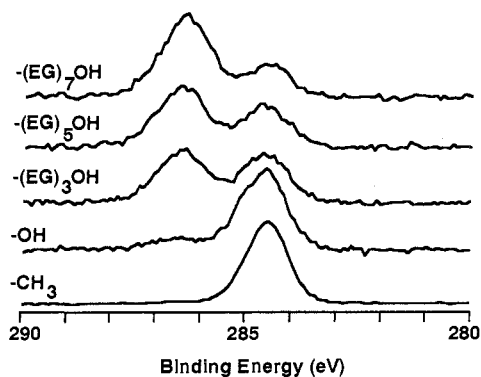


Figure 2. XPS of monolayers prepared from $\text{HS}(\text{CH}_2)_{11}\text{R}$ on gold: high-resolution spectra of the $\text{C}(1\text{s})$ region. Each spectrum is labeled by its R group.

vided the monoether.²³ Photochemical addition of thioacetic acid to the double bond gave the thioacetate in good yield.²⁴ To avoid oxidation of the thiol to the corresponding disulfide, methanolysis of the thioacetate was carried out in acid (0.1 M HCl in methanol) either at room temperature for 4–5 days or at reflux for 4 h; both procedures gave similar yields. Analysis by ^1H NMR spectroscopy indicated that disulfides were not present.²⁵

Preparation of SAMs. SAMs containing $\text{HS}-11-(\text{EG})_m\text{OH}$ were prepared from 1 mM solutions of the thiols dissolved in deoxygenated, absolute ethanol, by placing gold-coated wafers in the solutions for 24 h at room temperature.^{12,26} The contact angles measured for SAMs prepared by this method were indistinguishable from those of SAMs prepared by immersion for periods of up to 1 month.

Characterization of SAMs. Ellipsometry. The thickness (d) of the SAMs (measured by ellipsometry) is linear in m , the number of glycol units. A plot of d against m is a straight line with a slope of 2.7 Å per OCH_2CH_2 unit and an intercept of 12 Å for $m = 0$ (Figure 1). The thickness was calculated with use of a parallel, homogeneous, three-layer (air, monolayer, substrate) model with an assumed refractive index of 1.45 for the monolayer.²⁷ The refractive index for ethylene glycol is 1.43, that for hexa(ethylene glycol) is 1.46, and that for undecane is 1.42. Variations of this magnitude in the refractive index (1.45 ± 0.03) do not significantly affect the calculated values of thickness. The observed scatter in the data is ± 2 Å for most thiol systems.

The linear plot suggests a consistent incremental increase in the thicknesses of the monolayers as a function of the number of ethylene glycol units. The value for the slope of the line (2.7 Å per OCH_2CH_2 group) is $\sim 15\%$ lower than the value of 3.1 Å calculated for trans-extended chains of OCH_2CH_2 units tilted at an angle of 30° from the normal to the surface.¹⁵ The dotted line in Figure 1 shows the calculated thicknesses for these monolayers. The experimentally significant difference between the observed and calculated values of incremental thickness for OCH_2CH_2 units indicates that at least the oligo(ethylene glycol) portion of these SAMs deviates from the model of all-trans conformation and 30° cant.

XPS. The high-resolution photoelectron spectrum of the carbon 1s region shows two peaks: One at 284.5 eV is characteristic of the internal units of the polymethylene chain ($\text{CH}_2\text{CH}_2\text{CH}_2$); the second at 286.5 eV corresponds to methylene groups adjacent to an oxygen (OCH_2) (Figure 2). The relative intensity of this latter peak increases with the number of glycol units (m). The atten-

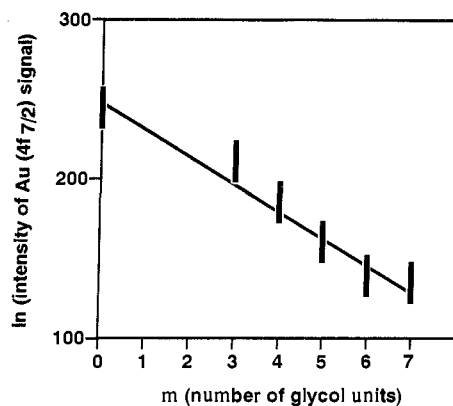


Figure 3. Intensity of the $\text{Au}(4f_{7/2})$ signal (in arbitrary units) measured by XPS as a function of the number of oligo(ethylene glycol) units in $\text{Au}-\text{S}-11-(\text{EG})_m\text{OH}$. The attenuation of the intensity as a function of m is compatible with an exponential dependence and suggests a consistent incremental increase in the thickness of the monolayer as a function of the number of ethylene glycol units.

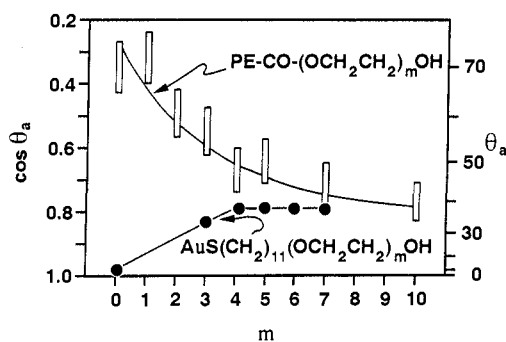


Figure 4. Wettability of oligo(ethylene glycol)-modified gold and polyethylene (PE) surfaces as a function of the numbers of ethylene glycol units (m). The point at $m = 0$ for derivatives of polyethylene is for $\text{PE}-\text{CH}_2\text{OH}$, not $\text{PE}-\text{CO}_2\text{H}$. Values of θ for $\text{Au}-\text{S}(\text{CH}_2)_{11}-(\text{OCH}_2\text{CH}_2)_m\text{OH}$ are the advancing contact angles of water; those for $\text{PE}-\text{CO}-(\text{OCH}_2\text{CH}_2)_m\text{OH}$ were measured by the sessile drop method. The roughness of the surface of PE causes the error in the measurement of contact angles on PE to be larger than those measured on Au.

Table 1. Contact Angles Measured on SAMs on Gold Obtained from $\text{HS}(\text{CH}_2)_{11}\text{R}^a$

R ^b	θ_a	θ_r	$\Delta \cos \theta^c$
CH_3	110	99	0.18
OH	10	<10	d
OCH_3^e	85 ^f	71 ^f	0.24
$(\text{CH}_2)_3\text{OCH}_3^f$	85	75	0.17
$(\text{EG})_3\text{OH}$	34	22	0.10
$(\text{EG})_4\text{OH}$	38	24	0.12
$(\text{EG})_5\text{OH}$	38	24	0.12
$(\text{EG})_6\text{OH}$	38	25	0.12
$(\text{EG})_7\text{OH}$	38	25	0.12

^a Advancing (θ_a) and receding (θ_r) static contact angles of water. ^b $(\text{EG})_m\text{OH} = -(\text{OCH}_2\text{OCH}_2)_m\text{OH}$. ^c $\Delta \cos \theta = \cos \theta_r - \cos \theta_a$. ^d The hysteresis is not a useful parameter when one or both contact angles is close to 0° . ^e Reference 12. ^f Laibinis, P. E.; Bain, C. D.; Whitesides, G. M. Unpublished results.

uation of the $\text{Au}(4f_{7/2})$ signal in this system is less than that for systems of comparable thickness composed of alkanethiolates.

Increasing the number of ethylene glycol units (m) exponentially attenuates the $\text{Au}(4f_{7/2})$ signal (Figure 3). This observation also suggests a consistent incremental increase in the thickness of the monolayer as a function of the number of ethylene glycol units.

Wetting. The value of the advancing contact angle of water ($\theta_a(\text{H}_2\text{O}) = 34\text{--}38^\circ$, Table 1) is higher than previously observed for thiol systems presenting only OH groups at the solid-liquid interface. A hydrophilic surface comprising densely packed polar groups (CH_2OH , CO_2H) has $\theta_a(\text{H}_2\text{O}) < 20^\circ$.¹² The relatively high values of $\theta_a(\text{H}_2\text{O})$ for these ethylene glycol containing SAMs

(23) Gibson, T. J. *Org. Chem.* **1980**, *45*, 1095.

(24) Cunneen, J. I. *J. Chem. Soc.* **1947**, 134.

(25) In the disulfides, the triplet methylene adjacent to sulfur is shifted upfield compared to the quartet methylene in the thiols. Dithiols were not present according to analysis by thin-layer chromatography.

(26) For complete experimental details, see: Troughton, E. B.; Bain, C. D.; Whitesides, G. M.; Nuzzo, R. G.; Allara, D. L.; Porter, M. D. *Langmuir* **1988**, *4*, 365.

(27) McCrackin, F. L.; Passaglia, E.; Stromberg, R. R.; Steinberg, H. L. *J. Res. Natl. Bur. Stand., Sect. A* **1963**, *67*, 363–377. Also: Wasserman, S. R. Ph.D. Thesis, Harvard University, 1988.

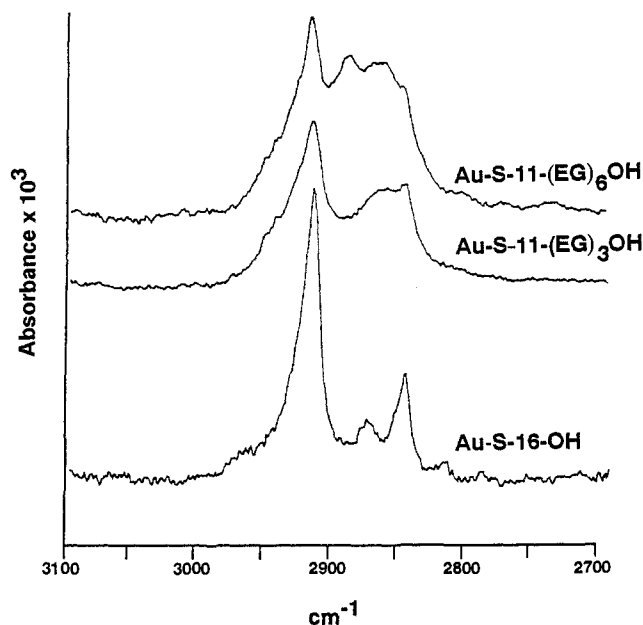


Figure 5. PIERS spectra of Au-S(CH₂)₁₁(OCH₂CH₂)₆OH, Au-S(CH₂)₁₁(OCH₂CH₂)₃OH, and Au-S(CH₂)₁₆OH. The broad feature at ~2880 cm⁻¹ in the spectrum of Au-S(CH₂)₁₆OH is due to the perturbation of the C-H stretching modes in the CH₂ group adjacent to the OH group (for further discussion, see ref 17). The spectra are shown stacked. The same scale of absorbance applies to all.

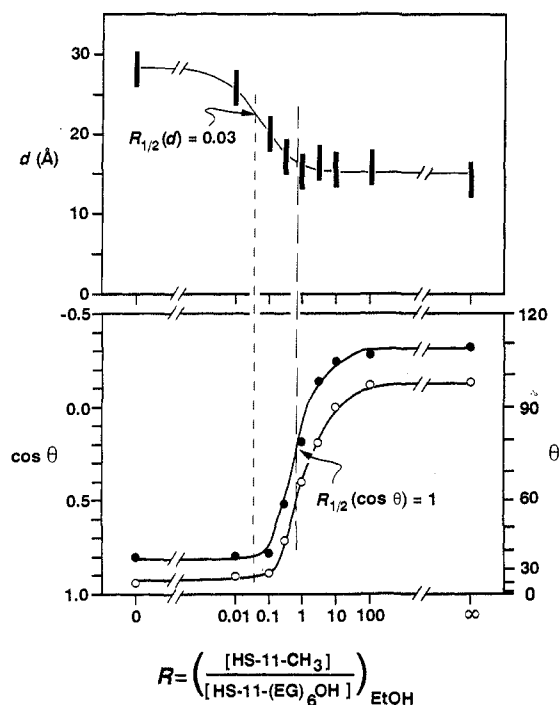


Figure 6. Competitive adsorption of HS-11-CH₃ and HS-11-(EG)₆OH onto gold from solution in ethanol: (top) ellipsometric thickness (d); (bottom) advancing (●) and receding (○) contact angles of water as a function of the relative concentration of the thiols in solution. The total concentration of thiol groups in deoxygenated, absolute ethanolic solution was 1 mM. SAMs were prepared by exposing the gold surface to the solution of thiols for 24 h at room temperature. The error in the contact angles is within the range of the points drawn. The dashed line --- is the midpoint in thickness ($R_{1/2}(d)$) and indicates approximately the value of R in solution yielding a 1:1 mixture of the two thiols on the resulting SAM; the dashed line - - - is the midpoint in $\cos \theta$ ($R_{1/2}(\cos \theta)$).

are consistent with an outer phase that exposes CH₂ groups to solution. This value is near the contact angle ($\theta_a(\text{H}_2\text{O}) = 40^\circ$) of a 1:1 mixed monolayer composed of HS(CH₂)₁₁OH and HS(CH₂)₁₉OH, where the outer phase is not closely packed.⁸ This

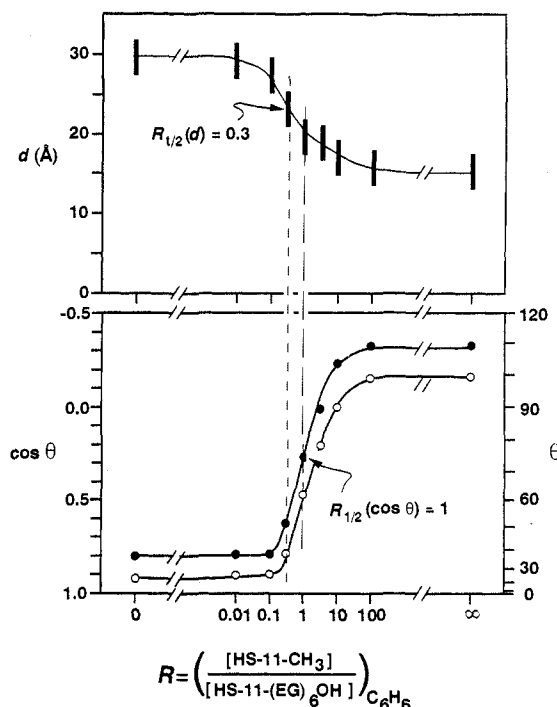


Figure 7. Competitive adsorption of HS-11-CH₃ and HS-11-(EG)₆OH onto gold from solution in benzene: (top) ellipsometric thickness; (bottom) advancing (●) and receding (○) contact angles as a function of the concentration in solution. The error in the contact angles is within the range of the points drawn. The caption to Figure 6 summarizes experimental parameters.

contact angle is also observed with a polyethylene film functionalized with oligo(ethylene glycol) esters (PE-CO-(OCH₂CH₂)_{*m*}OH when $m = 10-15$) (Figure 4).²⁸ We note, however, that the roughness of surface-modified polyethylene as well as disorder contributes to its wettability and apparent hydrophilicity, so direct comparison of contact angles measured on these surfaces to those of SAMs on gold is only qualitative.

Polarized Infrared External Reflectance Spectroscopy (PIERS). Analysis by PIERS gave spectra having broad and featureless peaks of absorbance in the C-H stretching region. There did appear to be a large peak at 2918 cm⁻¹, characteristic of crystalline or near-crystalline methylene groups, but this peak was partially obscured by other peaks. Figure 5 reproduces representative spectra.

Mixed Monolayers. We prepared monolayers containing mixtures of two thiols from ethanolic solutions containing mixtures of the two thiols. The mole fractions of the two adsorbates were varied while the total concentration of thiol in the solution was kept constant at 1 mM (Figures 6-9). This strategy has been shown previously to be a useful method of identifying the ratio of components in solution (R) that leads to a mixture of these components in the SAMs derived from them.^{29,30}

On plots of wettability ($\cos \theta$) and thickness (d) as a function of R (Figures 6-9), we indicate the midpoints for the changes in thickness and wettability from one extreme of the mixed monolayer to the other. We denote the value of R for the midpoint of the change in thickness as $R_{1/2}(d)$ and the value of R for the midpoint of the change in wettability as $R_{1/2}(\cos \theta)$. These two parameters provide useful points of calibration for discussing mixed monolayers.

SAMs Containing HS-11-CH₃ and HS-11-(EG)₆OH. The ellipsometric thicknesses of the monolayers formed by adsorption from ethanol decreased smoothly from 28 Å for pure HS-11-

(28) Holmes-Farley, S. R.; Bain, C. D.; Whitesides, G. M. *Langmuir* **1988**, *4*, 921.

(29) Bain, C. D.; Evall, J.; Whitesides, G. M. *J. Am. Chem. Soc.* **1989**, *111*, 7155.

(30) Bain, C. D.; Whitesides, G. M. *J. Am. Chem. Soc.* **1989**, *111*, 7164.

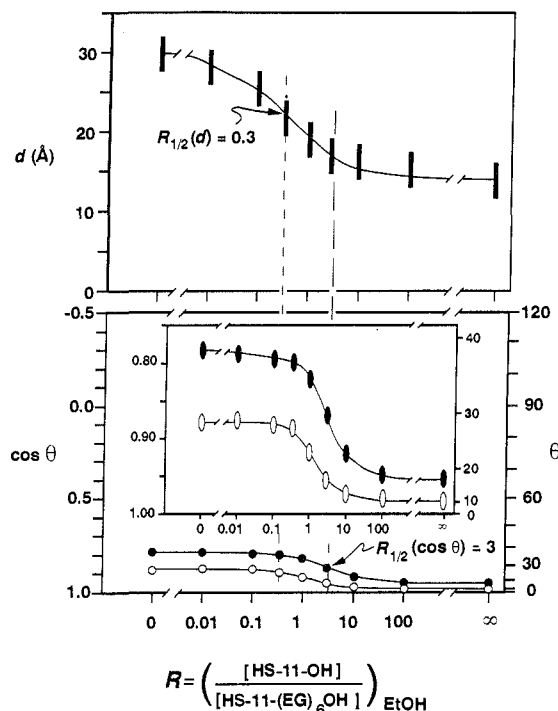


Figure 8. Competitive adsorption of HS-11-OH and HS-11-(EG)₆OH onto gold from solution in ethanol: (top) ellipsometric thickness; (bottom) advancing (●) and receding (○) contact angles as a function of the concentration in solution. The error in the contact angles is within the range of the points drawn. The caption to Figure 6 summarizes experimental parameters.

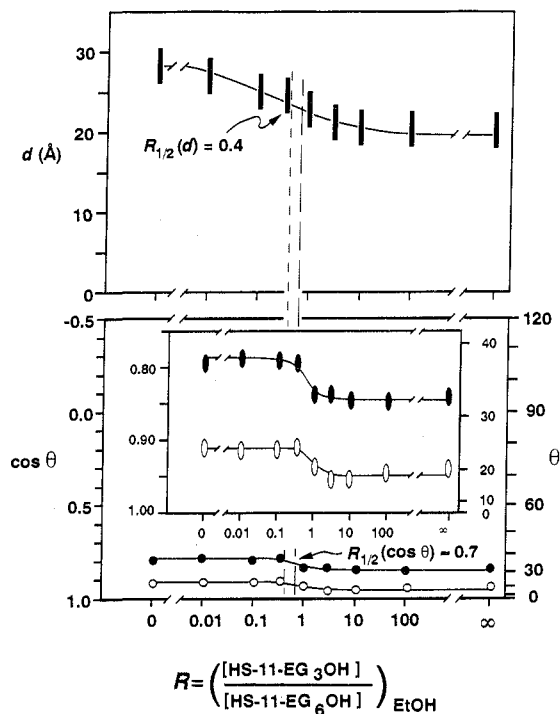


Figure 9. Competitive adsorption of HS-11-(EG)₃OH and HS-11-(EG)₆OH onto gold from solution in ethanol: (top) ellipsometric thickness; (bottom) advancing (●) and receding (○) contact angles as a function of the concentration in solution. The error in the contact angles is within the range of the points drawn. The caption to Figure 6 summarizes experimental parameters.

(EG)₆OH to 14 Å for pure HS-11-CH₃ in the region between $R = 0.01$ and $R = 1$ (Figure 6).

The compositions of the monolayers and of the solutions from which they were adsorbed were not the same. We presume that the midpoint in the thickness of the monolayers ($R_{1/2}(d)$) cor-

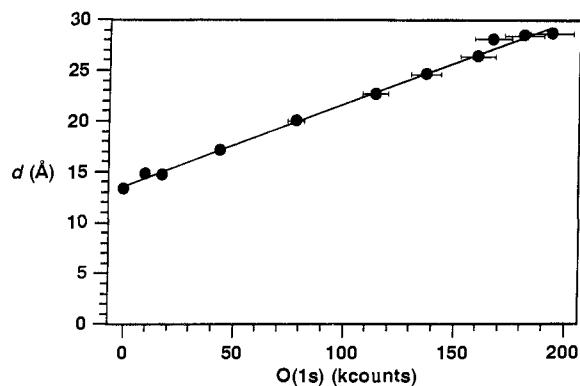


Figure 10. Thicknesses of a series of mixed SAMs of HS(CH₂)₁₀CH₃ and HS-11-(EG)₆OH, measured by ellipsometry, vs the intensities of the oxygen 1s X-ray photoelectron peaks of the same monolayers. The scatter in the ellipsometric measurements is contained within the data points; the horizontal error bars represent 5% of the O(1s) signal, the estimated accuracy of the XPS quantification techniques that were used. The degree of linearity is high: $r^2 > 0.995$.

responds to a SAM containing equal numbers of molecules of S-11-CH₃ and S-11-(EG)₆OH; this point occurred at $R = ([\text{HS-11-CH}_3]/[\text{HS-11-(EG)}_6\text{OH}])_{\text{EtOH}} = 0.03$. We have explicitly correlated thickness with composition in a closely related system. The measured ellipsometric thicknesses of mixed SAMs of HS-10-CH₃ and HS-11-(EG)₆OH correlate linearly ($r^2 > 0.995$) with the observed intensities of the O(1s) X-ray photoelectron spectra of these monolayers (Figure 10). This correlation strongly suggests the accuracy of ellipsometric thickness as a measure of composition in appropriately chosen SAMs containing two components.

The mole fraction of HS-11-(EG)₆OH in the monolayer was lower than the mole fraction in solution (by a factor of ~ 30); that is, chemisorption of HS-11-(EG)₆OH was less favorable than chemisorption of HS-11-CH₃. We have not established rigorously the origin of this partitioning. Possible contributing factors include unfavorable interactions between the EG chains in the monolayer, favorable solvation of these chains in the ethanol solution, and steric interactions during formation of the SAM. Chemisorption of HS-11-(EG)₆OH from solutions in benzene (a non-hydrogen-bonding solvent) was more favorable than chemisorption from ethanol: The value of $R_{1/2}(d)$ increased by an order of magnitude to 0.3 when SAMs were formed from benzene rather than ethanol (Figure 7). This result suggests that hydrogen bonding of the oligo(ethylene glycol) chains to ethanol reduces their tendency to form SAMs. Factors other than hydrogen bonding—e.g., differences in solubility or π -interactions—could, also, contribute to the change in $R_{1/2}(d)$.

Comparison of the curves of monolayer thickness and wettability as a function of R for the system comprised of HS-11-CH₃ and HS-11-(EG)₆OH adsorbed from ethanol shows an experimentally significant difference in the values of R at which the curves reach their midpoint ($R_{1/2}(d) = 0.03$ and $R_{1/2}(\cos \theta) = 1.0$). This observation suggests that a low extent of incorporation of HS-11-(EG)₆OH into a monolayer of HS-11-CH₃ has a much larger effect on wettability than on thickness. A possible interpretation of this result would be that one -(EG)₆OH group is sufficiently large and flexible that it "shields" several (~ 3) underlying CH₃ groups from interaction with water. This shielding might occur in two ways. The dilute -(EG)₆OH groups, solvated with water, could form a thin hydrogel over HS-11-CH₃. Alternatively, favorable hydrophobic interactions might cause the methylene groups of the EG chains to collapse onto the exposed methylene and methyl groups of HS-11-CH₃, and expose ether and hydroxyl groups preferentially at the solid-water interface.

The series of monolayers formed from HS-11-(EG)₆OH and HS-11-CH₃ by adsorption from benzene does *not* show as large a difference between $R_{1/2}(d)$ and $R_{1/2}(\cos \theta)$ as that from ethanol. The fact that $\cos \theta$ is significantly different for monolayers formed by adsorption from these different solvents at the same values of

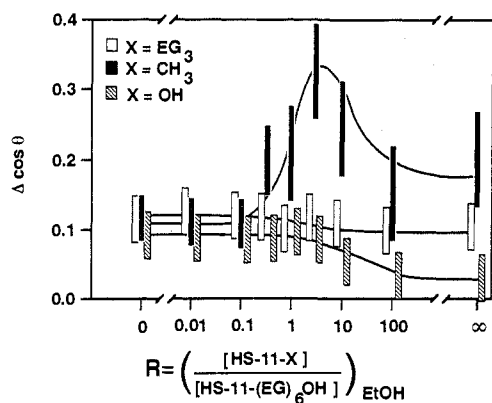


Figure 11. Hysteresis ($\Delta \cos \theta = \cos \theta_r - \cos \theta_a$) in the contact angle on mixed monolayers on gold. The data are derived from Figures 6–9. Data at each value of R are slightly horizontally displaced to avoid overlap.

d (that is, at the same composition of the monolayers) indicates that they must differ in some other way. The difference is in the direction expected if the S-11-(EG)₆OH moieties are clustered or form islands when adsorbed from benzene but are dispersed more uniformly among the S-11-CH₃ groups when adsorbed from ethanol.

SAMs Containing HS-11-OH and HS-11-(EG)₆OH. The ellipsometric thicknesses of the monolayers decreased smoothly from 28 Å for the SAM from pure HS-11-(EG)₆OH to 14 Å for the SAM from pure HS-11-OH (Figure 8). The midpoint in the plot of thickness versus R ($R_{1/2}(d)$) occurred at $R = 0.3$; that for $\cos \theta$ ($R_{1/2}(\cos \theta)$) occurred at $R \approx 3$. Again, the concentration of HS-11-(EG)₆OH in the monolayers was lower than that in the solutions from which the monolayers were formed. The same arguments suggested to rationalize the corresponding observations for HS-11-CH₃/HS-11-(EG)₆OH apply here.

SAMs Containing HS-11-(EG)₃OH and HS-11-(EG)₆OH. The ellipsometric thicknesses of the monolayers decreased from 28 Å for pure HS-11-(EG)₆OH to 20 Å for pure HS-11-(EG)₃OH in the region centered at $R \approx 0.4$ (Figure 9). As expected, $\cos \theta$ changed relatively little over this region. There was little difference in the values of $R_{1/2}(d)$ and $R_{1/2}(\cos \theta)$.

Hysteresis in Contact Angle. At least three factors contribute to hysteresis at nonreacting solid–liquid interfaces: heterogeneity of the surface, roughness of the surface, and the extent of microreconstruction of the surface under the drop.³¹ The hysteresis (12–14°) in the measured values of the contact angle for homogeneous monolayers was small for each system (Table I). This observation suggests that microreconstruction did not occur, or did not significantly affect the wettability of the surface. The magnitude of the hysteresis was similar to that observed for well-ordered SAMs of alkanethiolates on gold.²⁵ In systems of mixed monolayers containing hydroxyl-terminated thiols (HS-11-OH vs HS-11-(EG)₆OH and HS-11-(EG)₃OH vs HS-11-(EG)₆OH), the change in hysteresis from one extreme to another was smooth and nearly linear (Figure 11).

Adsorption of Proteins to SAMs. We examined the adsorption of proteins on three surfaces: Au–S-11-CH₃, Au–S-11-OH, and Au–S-11-(EG)₆OH. We exposed slides covered with SAMs to aqueous solutions of phosphate buffer (pH 7.5) containing a single protein (1 mg/mL) for 1 h at 25 °C, removed the slides, washed them with water, and used ellipsometry to measure changes in thickness. When the thickness of a monolayer increased, presumably due to the adsorption of protein onto its surface, analysis by XPS indicated the appearance of a nitrogen signal (Figure 12). The apparent thickness of SAMs prepared from solutions of HS-11-CH₃ showed experimentally significant increases in thickness of >20 Å following exposure to avidin, hexokinase, or pyruvate kinase. The apparent thickness of SAMs formed from HS-11-OH or HS-11-(EG)₆OH did not increase significantly

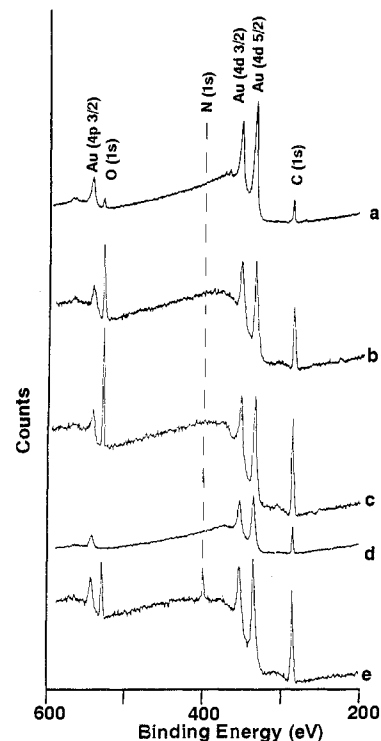


Figure 12. XPS spectra of (a) untreated gold, (b) Au–S-11-(EG)₆OH, (c) Au–S-11-(EG)₆OH after exposure to avidin, (d) Au–S-11-CH₃, (e) Au–S-11-CH₃ after exposure to avidin. Signal for nitrogen (presumably from the adsorption of avidin to the surface) is visible near 400 eV in spectrum e. Signals for C and O in (a) are from contaminants on untreated gold. Adsorption of thiols displaces these contaminants.

Table II. Increase in Thickness of SAMs on Gold after Contact with a Solution of Avidin (1 mg/mL) in 10 mM Phosphate Buffer for 1 h at 25 °C Followed by Rinsing with Water

surface (Au–S(CH ₂) ₁₁ R)	increase in thickness (Å) ^a
CH ₃	29 ± 2
OH	4 ± 8
(EG) ₆ OH	2 ± 2

^a The error represents the 95% confidence interval around the mean ($n = 5$).

following exposure to the same proteins, nor did the apparent thickness of SAMs formed from HS-11-(EG)₆OH increase after exposure to a 5% solution (pH 7.8) of adult chicken whole blood in Alsever solution.³² Table II gives representative data for the adsorption of avidin onto SAMs. There is more scatter in the data for SAMs of HS-11-OH than for HS-11-(EG)₆OH. This observation may reflect the different structures of the monolayers. SAMs formed from HS-11-OH expose only a single layer of hydroxyl groups to solution and, with regard to adsorption of proteins, may be more sensitive to defects that expose underlying methylene groups than are SAMs formed from HS-11-(EG)₆OH. The latter SAMs have a thicker outer hydrophilic layer than the former.

Discussion

Spontaneous self-assembly of functionalized alkanethiols on gold provides a route to surfaces presenting oligo(ethylene glycol) moieties at the solid–water interface. How well-organized are these SAMs?

Three types of evidence combine to suggest that these structures are monolayers—probably with the same density of adsorbed thiolate groups on the gold surface as with SAMs of *n*-alkanethiolates—with substantial disorder in the oligo(ethylene glycol) part of the monolayer. We have neither a direct measure of the

(31) Ferguson, G. S.; Whitesides, G. M. In *Modern Approaches to Wettability: Theory and Applications*; Loeb, G., Schrader, M., Eds.; in press.

(32) Alsever's solution is a solution of sodium citrate (40 mM), NaCl (70 mM), and dextrose (110 mM) in distilled water.

order in the $(\text{CH}_2)_n$ portions of these SAMs nor a valid means of comparing them with SAMs derived from structurally simpler precursors. In fact, we cannot presently define "order" quantitatively: We have no well-defined metric for "order", and relating the relevant observable physical and spectroscopic parameters—thickness, wettability, and IR spectra—to order is presently a qualitative process based on comparisons with better defined model systems.^{29,30}

The ellipsometric thicknesses of the SAMs containing S-11-(EG)_mOH moieties are compatible with complete coverage of the gold surface by these thiolates. The measured thicknesses are systematically less than those expected if the conformations of the (EG)_m moieties in the monolayers were strictly analogous to that of an *n*-alkyl moiety: all-trans with a cant angle of 30°. The densities of simple derivatives of ethylene glycol as liquids are higher than those of homologous alkanes by ~20% (presumably in part because the molar volume of an ether oxygen is less than that of a methylene group), and the -(EG)_mOH derivatives may be able to condense into a smaller molar volume than corresponding derivatives of -(CH₂)_{3m}OH.³³ This difference may be even more pronounced if hydrogen bonding between the terminal hydroxyl group and ether oxygen atoms is important. The difference in densities between derivatives of ethylene glycol and alkanes is compatible with the ~15% decrease in thickness of the OCH₂CH₂ portion of the SAM, relative to the thickness expected for a trans-extended structure.

In summary, the ellipsometric data are compatible with, but do not demand, a model for SAMs of S-11-(EG)_mOH in which the adsorbed sulfur atoms have the same surface density as those in homologous SAMs of composition S(CH₂)_{11+3m}OH, but in which the lower molar volumes of the (EG)_mOH groups, relative to those of the (CH₂)_{3m}OH groups, permit ~15% condensation in volume of the oxygen-containing portion of the monolayer when it is dry and penetration of this part of the monolayer by water when it is wet.

PIERS has been extraordinarily useful in defining the conformations of (CH₂)_n units in SAMs.^{13,17} Its utility is, unfortunately, limited for the SAMs of interest here because the CH₂ groups of the EG moieties provide broad, intense absorption. These latter absorptions are themselves not easily interpretable.³⁵

The wettability of the SAMs containing S-11-(EG)_mOH groups is interpretable qualitatively in terms of a disordered monolayer-water interface. These monolayers are substantially more hydrophobic than monolayers derived from molecules with composition HS(CH₂)_nOH. The most plausible explanation for this difference is that the latter SAMs are the more highly ordered and present a uniform array of CH₂OH groups at the solid-water interface, while the SAMs terminated with (EG)_mOH groups present a mixture of -CH₂OH and the more hydrophobic -CH₂OCH₂- groups. We cannot justify more detailed interpretation of the wettability of SAMs derived from HS-11-(EG)_mOH beyond that attributing disorder to the (EG)_mOH group other than noting that the wettability is similar for *m* = 3–7 and that if the suggestion of disorder in these systems is correct, they are probably swollen when in contact with water.

Two additional features of these monolayers provide information about their structure.

The first observation is that comparison of the values of $R_{1/2}(d)$ (Figures 6–9) establishes that it is favorable for the *shorter* alkanethiols to adsorb on the gold relative to HS-11-(EG)₆OH. In contrast, for unfunctionalized alkanethiols and for HS(CH₂)_nOH adsorption of the *longer* chain species is favored.³⁰ This result implies that it is relatively difficult to transfer the -(EG)₆OH moiety from the ethanol solution to the microenvironment of the

SAM. The fact that it is more favorable to adsorb HS-11-(EG)₆OH onto gold from solutions of benzene rather than of ethanol suggests this difficulty reflects the loss of hydrogen bonding or conformational entropy in the SAM.

The second observation concerns the substantial difference in the values of $R_{1/2}(\cos \theta)$ and $R_{1/2}(d)$ of the mixed monolayer of S-11-CH₃ and S-11-(EG)₆OH prepared by adsorption from ethanol solution (Figure 6) (but *not* from benzene, Figure 7). A small extent of incorporation of the EG-containing component onto the monolayer (~10%) produces a large change (50%) in the wettability of the monolayer. Thus, a single (EG)₆OH moiety appears to be able to prevent several—perhaps 3—surface methyl (or CH₂OH, Figure 8) groups in its vicinity from interacting with water in a way that influences contact angle.^{35,36}

The qualitative picture of the structure of these SAMs that emerges from this study is one in which the SAMs derived from pure derivatives of HS-11-(EG)_mOH probably consist of two-layer structures—a -(CH₂)₁₁- layer and a -(EG)_mOH layer. Whether the -(CH₂)₁₁- is as ordered as corresponding layers in simpler derivatives is not defined by this work. The outer (EG)_mOH layer is probably disordered when in contact with water.

In a preliminary survey, we found that proteins adsorbed to hydrophobic SAMs that were formed from HS-11-CH₃ but adsorbed significantly more weakly to relatively hydrophilic surfaces that were formed from HS-11-OH or HS-11-(EG)₆OH. We emphasize that the term "protein adsorption" in the context of this paper is interpretable only with respect to the specific experimental protocol used; we detected only adsorption strong enough to survive the procedure for washing. Although these experiments of protein adsorption addressed an experimental system of minimal complexity, they achieved one goal of this work: to demonstrate the practicality of using SAMs prepared by adsorption of thiols on gold as model substrates for studying the adsorption of proteins onto organic surfaces. Since this class of SAMs provides the most ordered, best understood, and most easily controlled surfaces now available in organic chemistry, the success of these first experiments demonstrates the practicality of this approach and indicates a route toward more realistic studies with more complex systems.

Experimental Section

Materials. Absolute ethanol (U.S. Industrials Co.) was purged with either argon or nitrogen for 1 h before use as a solvent for the preparation of SAMs. Deionized water was distilled from glass in a Corning Ag-1b still.

1-Dodecanethiol (Aldrich, 98%), 11-bromo-1-undecene (Pfaltz and Bauer), tri(ethylene glycol) (Aldrich, 98%), tetra(ethylene glycol) (Fluka, >97%), penta(ethylene glycol) (Lancaster, 99%), hexa(ethylene glycol) (Aldrich, 98%), hepta(ethylene glycol) (Aldrich, 97%), and thioacetic acid (Fluka 97%) were used as received. 11-Mercapto-1-undecanol was available from previous studies.¹²

¹H NMR and ¹³C spectra were obtained at 300 or 250 MHz and were referenced to chloroform.

Preparation and Handling of Gold Substrates. Gold substrates were prepared by electron-beam evaporation of ~2000 Å of high-purity gold (99.999%) onto 100-mm single-crystal silicon wafers that had been precoated with chromium to improve adhesion (50–100 Å of Cr followed by 2000 Å of Au). The gold-coated wafers were stored in polypropylene wafer holders (Fluoroware) and used as soon as possible after being exposed to the atmosphere. Before use, the gold-coated wafers were cut into pieces ~1 cm × 3 cm with a diamond-tipped stylus, rinsed with ethanol, and blown dry with a stream of nitrogen. Glassware was thoroughly cleaned, rinsed with copious amounts of distilled water, and

(33) The densities (ρ , g cm⁻³) of simple oligo(ethylene glycol) compounds are higher than those of alkanes: CH₃OCH₂CH₂OH, 0.965; HOCH₂CH₂OCH₂CH₃, 0.930; CH₃OCH₂CH₂OCH₂CH₃, 0.937; HOCH₂CH₂OCH₂CH₂OCH₂CH₃, 0.999; CH₃CH₂OCH₂CH₂OCH₂CH₂OCH₂CH₃, 0.909; CH₃C₆H₄OCH₂CH₂OCH₂CH₂OCH₂CH₂CH₃, 0.855; *n*-C₈H₁₈, 0.659; *n*-C₁₈H₃₈, 0.777.

(34) Preparation and analysis of deuterated compounds (e.g., HS-11-O-(CD₂CD₂)_nOH) could simplify the interpretation of the IR spectra.

(35) For discussions of the steric stabilization of colloids composed of particles having oligo(ethylene glycol) chains on their surfaces, see: Sato, T.; Ruch, R. *Stabilization of Colloidal Dispersions by Polymer Adsorption*; Marcel Dekker: New York, 1980. Napper, D. H. *J. Colloid Interface Sci.* **1977**, *58*, 390. Cowell, C.; Li-In-On, R.; Vincent, B. *J. Chem. Soc., Faraday Trans. 1* **1978**, *74*, 337. Vold, R. D.; Vold, M. J. *Colloid and Interface Chemistry*; Addison-Wesley: Reading, MA, 1983; 275–281.

(36) We are examining this same phenomenon with pendant oligo-saccharide chains. These chains are more hydrophilic, but also larger and more rigid than the oligo(ethylene glycol) chains. A comparison of oligo-saccharide- and oligo(ethylene glycol)-containing systems should help to disentangle contributions to the shielding of surfaces of SAMs on gold.

then soaked in freshly prepared "piranha" solution (7:3 v/v mixture of concentrated H₂SO₄ and 30% aqueous H₂O₂) for 1 h, followed by exhaustive rinsing with distilled water, a final rinsing with absolute ethanol, and drying in an oven. (Caution: "piranha" solution reacts violently with many organic materials and should be handled with extreme care.)

Solutions used in the preparation of SAMs containing two thiols were prepared in glass weighing bottles by diluting 5 mM stock solutions. The accuracy of the concentrations of the stock solutions ($\pm 5\%$) was limited by the analytical balance used. An Eppendorf micropipet was used to transfer solutions (contributing an error of <1% in the final concentration). The total concentration of thiol in the solution was 1 mM. Gold slides were washed with ethanol, blown dry with a stream of nitrogen, and immersed in freshly prepared solutions overnight at room temperature.

Contact Angles. Contact angles were determined at ambient laboratory temperatures (17–22 °C) with a Ramé-Hart Model 100 contact angle goniometer. Probe liquids were dispensed from a Matrix Technologies Micro-electrapipette. Measurement of contact angles is described elsewhere.²⁶ Reported values are the average of at least five measurements, taken at different locations on the surface.

Ellipsometry. Ellipsometric measurements were made with a Rudolf Research Type 43603-200E thin-film ellipsometer with a wavelength of 6328 Å (He-Ne laser) and an incident angle of 70°. Samples were washed with ethanol and blown dry with nitrogen before optical constants were measured. Readings were taken on clean gold to establish the bare substrate optical constants and after monolayer formation. Three separate values of thickness were measured on each sample, and the values were then averaged. Thicknesses were computed with a planar three-layer (ambient, monolayer, substrate) isotropic model with assumed refractive indices of 1.00 and 1.45 for the ambient and monolayer, respectively.²⁷

X-ray Photoelectron Spectroscopy (XPS). XPS spectra were obtained on an SSX-100 spectrometer (Surface Science Instruments) equipped with an Al K α source, quartz monochromator, concentric hemispherical analyzer in transmission mode, and a multichannel detector. The take-off angle was 35°, and the operating pressure was approximately 5×10^{-9} Torr. All spectra were referenced to Au(4f_{7/2}) at 84.00 eV. The diameter of the spot size for all spectra was 1000 μ m. Spectra were fitted with an 80% Gaussian/20% Lorentzian function with the Surface Science Instruments software.

Syntheses of HS-(CH₂)₁₁-Oligo(ethylene glycols). **Undec-1-en-11-yltri(ethylene glycol) (1).** A mixture of 0.34 mL of 50% aqueous sodium hydroxide (4.3 mmol) and 3.2 g of tri(ethylene glycol) (21 mmol) was stirred for about 0.5 h in an oil bath at 100 °C under an atmosphere of argon, and then 1.0 g of 11-bromoundec-1-ene (4.3 mmol) was added. After 24 h, the reaction mixture was cooled and extracted six times with hexane. Concentration of the combined hexane portions by rotary evaporation at reduced pressure gave a yellow oil containing a mixture of mono- and diethers, according to analysis by ¹H NMR spectroscopy. Purification of the oil by chromatography on silica gel (eluant: ethyl acetate) gave 0.98 g of monoether **1**: 76% yield; ¹H NMR (250 MHz, CDCl₃) δ 1.2 (br s, 12 H), 1.55 (qui, 2 H, $J = 7$ Hz), 2.0 (q, 2 H, $J = 7$ Hz), 2.7 (br s, 1 H), 3.45 (t, 2 H, $J = 7$ Hz), 3.5–3.8 (m, 12 H), 4.9–5.05 (m, 2 H), 5.75–5.85 (m, 1 H).

Undec-1-en-11-yltetra(ethylene glycol) (2). Reaction of 10 equiv of tetra(ethylene glycol) and 1 equiv of 11-chloroundec-1-ene as described for **1** gave **2**: 63% yield; ¹H NMR (250 MHz, CDCl₃) δ 1.3 (br s, 12 H), 1.55 (qui, 2 H, $J = 7$ Hz), 2.0 (q, 2 H, $J = 7$ Hz), 2.85 (br s, 1 H), 3.4 (t, 2 H, $J = 7$ Hz), 3.5–3.75 (m, 16 H), 4.9–5.05 (m, 2 H), 5.75–5.85 (m, 1 H); IR (neat) ν_{\max} 3450, 2900, 2840, 1100 cm⁻¹.

Undec-1-en-11-ylpenta(ethylene glycol) (3). Compound **3** was prepared as described for **1** with one exception: The eluant for the chromatography step was ethyl acetate, followed by MeOH/CHCl₃ (1:19 and then 1:9): 78% yield; ¹H NMR (250 MHz, CDCl₃) δ 1.2 (br s, 12 H), 1.55 (qui, 2 H, $J = 7$ Hz), 2.0 (q, 2 H, $J = 7$ Hz), 2.85 (br s, 1 H), 3.4 (t, 2 H, $J = 7$ Hz), 3.5–3.75 (m, 20 H), 4.9–5.05 (m, 2 H), 5.75–5.85 (m, 1 H).

Undec-1-en-11-ylhexa(ethylene glycol) (4). Compound **4** was prepared as described for **3**: 78% yield; ¹H NMR (250 MHz, CDCl₃) δ 1.25 (br s, 12 H), 1.55 (qui, 2 H, $J = 7$ Hz), 1.7 (br s, 1 H), 2.05 (q, 2 H, $J = 7$ Hz), 3.45 (t, 2 H, $J = 7$ Hz), 3.55–3.75 (m, 24 H), 4.9–5.05 (m, 2 H), 5.75–5.85 (m, 1 H); IR (neat) ν_{\max} 3450, 2920, 2850, 1100 cm⁻¹.

Undec-1-en-11-ylhepta(ethylene glycol) (5). Reaction of 3 equiv of hepta(ethylene glycol) and 1 equiv of 11-chloroundec-1-ene as described for **3** gave **5**: 87% yield; ¹H NMR (250 MHz, CDCl₃) δ 1.2 (br s, 12 H), 1.5 (qui, 2 H, $J = 7$ Hz), 2.0 (q, 2 H, $J = 7$ Hz), 2.75 (br s, 1 H), 3.5 (t, 2 H, $J = 7$ Hz), 3.5–3.75 (m, 28 H), 4.9–5.05 (m, 2 H), 5.75–5.85 (m, 1 H).

General Syntheses of [1-[(Methylcarbonyl)thio]undec-11-yl]oligo(ethylene glycol). Solutions of the olefins (200–400 mM) in MeOH

containing 2–4 equiv of thioacetic acid and 5–10 mg of AIBN were irradiated for 4–6 h under an atmosphere of nitrogen with a 450-W, medium-pressure mercury lamp (Ace Glass) filtered through Pyrex. Concentration of the reaction mixtures by rotary evaporation at reduced pressure followed by purification by chromatography on silica gel gave the thioacetates in 78–88% yields.

[1-[(Methylcarbonyl)thio]undec-11-yl]tri(ethylene glycol): ¹H NMR (250 MHz, CDCl₃) δ 1.25 (br s, 14 H), 1.6 (m, 4 H), 2.3 (s, 3 H), 2.85 (t, 2 H, $J = 7$ Hz), 3.45 (t, 2 H, $J = 7$ Hz), 3.5–3.75 (m, 12 H).

[1-[(Methylcarbonyl)thio]undec-11-yl]tetra(ethylene glycol): ¹H NMR (250 MHz, CDCl₃) δ 1.25 (br s, 15 H), 1.6 (m, 4 H), 2.3 (s, 3 H), 2.85 (t, 2 H, $J = 7$ Hz), 3.45 (t, 2 H, $J = 7$ Hz), 3.5–3.75 (m, 16 H).

[1-[(Methylcarbonyl)thio]undec-11-yl]penta(ethylene glycol): ¹H NMR (250 MHz, CDCl₃) δ 1.25 (br s, 14 H), 1.55 (m, 4 H), 2.3 (s, 3 H), 2.85 (t, 2 H, $J = 7$ Hz), 2.9 (br s, 1 H), 3.45 (t, 2 H, $J = 7$ Hz), 3.55–3.75 (m, 20 H).

[1-[(Methylcarbonyl)thio]undec-11-yl]hexa(ethylene glycol): ¹H NMR (300 MHz, CDCl₃) δ 1.25 (br s, 14 H), 1.5 (m, 4 H), 2.3 (s, 3 H), 2.4 (br s, 1 H), 2.8 (t, 2 H, $J = 7$ Hz), 3.4 (t, 2 H, $J = 7$ Hz), 3.5–3.7 (m, 24 H).

[1-[(Methylcarbonyl)thio]undec-11-yl]hepta(ethylene glycol): ¹H NMR (250 MHz, CDCl₃) δ 1.25 (br s, 14 H), 1.6 (m, 4 H), 2.3 (s, 3 H), 2.8 (br s, 1 H), 2.85 (t, 2 H, $J = 7$ Hz), 3.45 (t, 2 H, $J = 7$ Hz), 3.55–3.75 (m, 28 H).

General Syntheses of (1-Mercapto)undec-11-yl)oligo(ethylene glycol). Solutions of the thioacetates in 0.1 M HCl in MeOH were deprotected under an atmosphere of nitrogen by refluxing for 4 h (**6**, **7**, **9**) or by stirring at room temperature for 4–5 days (**8**, **10**). Concentration of the reaction mixtures by rotary evaporation at reduced pressure followed by purification of the residues by chromatography on silica gel gave the thiols in 84–91% yields.

(1-Mercapto)undec-11-yl)tri(ethylene glycol) (HS-11-(EG)₃OH, 6): ¹H NMR (250 MHz, CDCl₃) δ 1.1 (br s, 14 H), 1.2 (t, 1 H, $J = 7$ Hz), 1.5 (m, 4 H), 2.5 (q, 2 H, $J = 7$ Hz), 3.0 (br s, 1 H), 3.4 (t, 2 H, $J = 7$ Hz), 3.5–3.75 (m, 12 H); ¹³C NMR (62 MHz, CDCl₃) δ 24.52 (t), 25.97 (t), 28.27 (t), 28.96 (t), 29.39 (t), 29.47 (t), 33.93 (t, CH₂SH), 61.54 (t, CH₂OH), 69.87 (t), 69.87 (t), 70.19 (t), 70.43 (t), 71.39 (t), 72.47 (t); IR (neat) ν_{\max} 3450, 2920, 2840, 2550, 1460, 1350, 1280, 1240, 1120, 930, 880 cm⁻¹; HRMS (FAB) for C₁₇H₃₆SO₄ calcd 336.2334, found 336.2362. Anal. Calcd for C₁₇H₃₆SO₄: C, 60.67; H, 10.79. Found: C, 60.59; H, 10.49.

(1-Mercapto)undec-11-yl)tetra(ethylene glycol) (HS-11-(EG)₄OH, 7): ¹H NMR (250 MHz, CDCl₃) δ 1.2 (br s, 14 H), 1.3 (t, 1 H, $J = 7$ Hz), 1.5 (m, 4 H), 2.5 (q, 2 H, $J = 7$ Hz), 2.85 (br s, 1 H), 3.4 (t, 2 H, $J = 7$ Hz), 3.55–3.75 (m, 16 H); ¹³C NMR (75 MHz, CDCl₃) δ 24.76 (t), 26.21 (t), 28.50 (t), 29.19 (t), 29.67 (t), 29.76 (t), 34.15 (t, CH₂SH), 61.80 (t, CH₂OH), 70.13 (t), 70.45 (t), 70.66 (t), 70.71 (t), 71.58 (t), 72.62 (t); HRMS (FAB) for C₁₉H₄₀SO₅, calcd 380.2596, found 380.2498. Anal. Calcd for C₁₉H₄₀SO₅: C, 59.96; H, 10.59. Found: C, 59.87; H, 10.47.

(1-Mercapto)undec-11-yl)penta(ethylene glycol) (HS-11-(EG)₅OH, 8): ¹H NMR (250 MHz, CDCl₃) δ 1.3 (br s, 14 H), 1.32 (t, 1 H, $J = 7$ Hz), 1.6 (m, 4 H), 2.3 (br s, 1 H), 2.5 (q, 2 H, $J = 7$ Hz), 3.45 (t, 2 H, $J = 7$ Hz), 3.5–3.80 (m, 20 H); ¹³C NMR (75 MHz, CDCl₃) δ 24.61 (t), 26.10 (t), 28.36 (t), 28.52 (t), 29.04 (t), 29.23 (t), 29.47 (t), 29.66 (t), 34.02 (t, CH₂SH), 61.85 (t, CH₂OH), 70.16 (t), 70.46 (t), 70.72 (t), 71.58 (t), 72.60 (t). Anal. Calcd for C₂₁H₄₄SO₆: C, 59.39; H, 10.45. Found: C, 59.55; H, 10.52.

(1-Mercapto)undec-11-yl)hexa(ethylene glycol) (HS-11-(EG)₆OH, 9): ¹H NMR (250 MHz, CDCl₃) δ 1.25 (br s, 14 H), 1.35 (t, 1 H, $J = 7$ Hz), 1.6 (m, 4 H), 2.5 (q, 2 H, $J = 7$ Hz), 2.7 (br s, 1 H), 3.45 (t, 2 H, $J = 7$ Hz), 3.55–3.75 (m, 24 H); ¹³C NMR (75 MHz, CDCl₃) δ 24.58 (t), 26.07 (t), 28.34 (t), 29.02 (t), 29.22 (t), 29.46 (t), 29.63 (t), 34.00 (t, CH₂SH), 61.77 (t, CH₂OH), 70.07 (t), 70.39 (t), 70.61 (t), 71.50 (t), 72.50 (t); IR (neat) ν_{\max} 3450, 2920, 2840, 2550, 1460, 1350, 1280, 1240, 1120, 930, 880 cm⁻¹; HRMS (FAB) for C₂₃H₄₈SO₇, calcd 468.3120, found 468.3093. Anal. Calcd for C₂₃H₄₈SO₇: C, 58.94; H, 10.33. Found: C, 58.89; H, 10.07.

(1-Mercapto)undec-11-yl)hepta(ethylene glycol) (HS-11-(EG)₇OH, 10): ¹H NMR (250 MHz, CDCl₃) δ 1.25 (br s, 14 H), 1.35 (t, 1 H, $J = 7$ Hz), 1.5 (m, 4 H), 2.5 (q, 2 H, $J = 7$ Hz), 2.65 (br s, 1 H), 3.45 (t, 2 H, $J = 7$ Hz), 3.55–3.75 (m, 28 H); ¹³C NMR (75 MHz, CDCl₃) δ 6.28 (t), 28.52 (t), 28.54 (t), 29.04 (t), 29.22 (t), 29.65 (t), 29.71 (t), 29.83 (t), 34.20 (t, CH₂SH), 61.97 (t, CH₂OH), 70.27 (t), 70.59 (t), 70.81 (t), 71.74 (t), 72.72 (t); HRMS (FAB) for C₂₅H₅₂SO₈, calcd 512.3383, found 512.3351. Anal. Calcd for C₂₅H₅₂SO₈: C, 58.56; H, 10.23. Found: C, 58.42; H, 10.07.

Measurements of Protein Adsorption. SAMs were washed with ethanol and then water, and their thicknesses were measured by ellipsometry. Slides were placed in a solution of protein (1 mg/mL) in 10 mM

phosphate buffer (pH 7.5) for 1 h at 25 °C. Slides then were removed, washed with 10 mL of water, mounted on the ellipsometer, and allowed to dry before their thickness was measured. At least three measurements were taken on each slide and averaged; the data reported in Table II represent the average increase in thickness of five slides.

Acknowledgment. We thank Gregory Ferguson (Lehigh

University), Hans Biebuyck and Yen-Ho Chu (Harvard University) for valuable discussions, and Paul Laibinis and John Folkers (Harvard University) for thorough readings of the manuscript. We thank Heather Nimmons (Boston University) for performing mass spectral analyses and Ralph Nuzzo (AT&T Bell Laboratories) for acquiring the PIERS data.

Detection and Characterization of Exchangeable Protons Bound to the Hydrogen-Activation Nickel Site of *Desulfovibrio gigas* Hydrogenase: A ^1H and ^2H Q-Band ENDOR Study

Chaoliang Fan,[†] Miguel Teixeira,[‡] Jose Moura,[‡] Isabel Moura,[‡] Boi-Hanh Huynh,[§] Jean Le Gall,[⊥] Harry D. Peck, Jr.,[⊥] and Brian M. Hoffman^{*†}

Contribution from the Department of Chemistry, Northwestern University, Evanston, Illinois 60208, Centro de Quimica Estrutural & Universidad Nova de Lisboa, 1096 Lisboa, Portugal, Department of Physics, Emory University, Atlanta, Georgia 30322, and Department of Biochemistry, University of Georgia, Athens, Georgia 30602.
Received May 5, 1989

Abstract: This paper presents a Q-band ENDOR study of the nickel site of the as-isolated (Ni-A), H₂-reduced (Ni-C), and reoxidized (Ni-A/Ni-B) states of *Desulfovibrio gigas* hydrogenase. Through proton and deuterium ENDOR measurements we detect and characterize the possible products of heterolytic cleavage of H₂, namely two distinct types of exchangeable protons, bound to the Ni-C site. One proton, H(1), has a hyperfine coupling, $A^{\text{H}}(1) = 16.8$ MHz and appears to interact directly with Ni-C. The other proton, H(2), has $A^{\text{H}}(2) \approx 4.4$ MHz and could be associated with H₂O or OH⁻ bound to nickel. We discuss possible binding modes for H(1) and H(2). One type of exchangeable deuterium(s), D(2), associated with the Ni-C center remains associated with the Ni-B center after oxidation of the Ni-C. In addition we confirm that the Ni-A site is inaccessible to solvent protons.

Introduction

The hydrogenase from *Desulfovibrio (D.) gigas* is composed of two subunits (26 and 63 kDa) and contains one nickel center, one [3Fe-4S], and two [4Fe-4S] clusters.^{1,2} It is currently believed that the nickel center is the substrate binding site. As isolated, the enzyme is catalytically inactive, and the nickel center exhibits an intense EPR signal, termed Ni-signal A ($g = 2.31, 2.26,$ and 2.02), and a weak signal, termed Ni-signal B ($g = 2.33, 2.16,$ and 2.02). Both of these are assigned to a formally trivalent, Ni(III) species, with the odd electron in the d_{z^2} orbital. Upon reduction by hydrogen, both signals disappear and a new nickel signal, termed Ni-signal C ($g = 2.19, 2.14,$ and 2.02), is observed. The g values of the Ni-signal C ($g_x \neq g_y > g_z \approx 2$) suggest that its unpaired electron also is associated with the d_{z^2} orbital of the nickel. However, whether the oxidation state of Ni-C is Ni(I) or Ni(III) is still in debate.³ Upon reoxidation, both Ni-signals A and B appear again with the relative intensity of the Ni-signal B increased.

In correlation with studies of catalytic activity, it has been concluded that the Ni-signals A and B represent inactive states of enzyme,^{4,5} and, in fact, some Ni-containing hydrogenases do not show these signals.⁶ The Ni-signal C, on the other hand, is observed in all the Ni-containing hydrogenases and is considered to represent a key intermediate in the catalytic cycle.^{5b,7} In support of these views, a recent electron spin echo study⁸ has shown that the nickel site is inaccessible to solvent protons in the Ni-A state but is accessible in the Ni-C state. However, characterization of the exchangeable protons associated with Ni-C was not possible.

Kinetic studies^{9,10} suggest that hydrogen activation by hydrogenase involves heterolytic cleavage of H₂, with the possible formation of a metal hydride species as an intermediate state. There has been no direct evidence for a metal hydride, but the results of photolyzing the reduced enzyme led to the proposal that the Ni-signal C represents such a species.^{11,12}

(1) Fauque, G.; Peck, H. D., Jr.; Moura, J. J. G.; Huynh, B. H.; Berlier, Y.; DerVartanian, D. V.; Teixeira, M.; Przybyla, A. E.; Lespinat, P. A.; Moura, I.; LeGall, J. *FEMS Microbiol. Rev.* **1988**, *54*, 299–344.

(2) Huynh, B. H.; Patil, D. S.; Moura, I.; Teixeira, M.; Moura, J. J. G.; DerVartanian, D. V.; Czechowski, M. H.; Prickril, B. C.; Peck, H. D., Jr.; LeGall, J. *J. Biol. Chem.* **1987**, *262*, 795–800.

(3) The Ni(I) assignment (d^9) requires that the $d_{x^2-y^2}$ orbital is lower in energy than the d_{z^2} orbital ("axial compression"), whereas the two orbitals would have a reverse order for Ni(III) (d^7 , "axial elongation"). In this paper, we make no attempt to address the issue of the Ni-C oxidation state. Instead, we only consider the Ni-C site as having an unpaired electron that occupies the d_{z^2} orbital. For a detailed discussion of the EPR of d^7 and d^9 systems, see: Salerno, J. C. In *Bioinorganic Chemistry of Nickel*; Lancaster, J. R. Jr., Ed.; VCH Publishers: Deerfield Beach, FL, USA, 1988; pp 53–71.

(4) Teixeira, M.; Moura, I.; Xavier, A. V.; Huynh, B. H.; DerVartanian, D. V.; Peck, H. D., Jr.; LeGall, J.; Moura, J. J. G. *J. Biol. Chem.* **1985**, *260*, 8942–8950.

(5) (a) Cammack, R.; Fernandez, V. M.; Schneider, K. In *Bioinorganic Chemistry of Nickel*; Lancaster, J. R. Jr., Ed.; VCH Publishers, Deerfield Beach, FL, USA, 1988; pp 167–189. (b) Fernandez, V. M.; Hatchikian, E. C.; Cammack, R. *Biochim. Biophys. Acta* **1985**, *832*, 69–79.

(6) Teixeira, M.; Fauque, G.; Moura, I.; Lespinat, P. A.; Berlier, Y.; Prickril, B.; Peck, H. D., Jr.; Xavier, A. V.; LeGall, J.; Moura, J. J. G. *Eur. J. Biochem.* **1987**, *167*, 47–58.

(7) Cammack, R.; Patil, D.; Fernandez, V. M. *Biochem. Soc. Trans.* **1985**, *13*, 572–578.

(8) Chapman, A.; Cammack, R.; Hatchikian, C. E.; McCracken, J.; Peisach, J. *FEBS Lett.* **1988**, *242*, 134–138.

(9) Krasna, A. L.; Rittenberg, D. *J. Am. Chem. Soc.* **1954**, *76*, 3015.

(10) Fauque, G. D.; Berlier, Y. M.; Czechowski, M. H.; Dimon, B.; Lespinat, P. A.; LeGall, J. *J. Ind. Microbiol.* **1987**, *1*, 1–9.

(11) Cammack, R.; Patil, D. S.; Hatchikian, E. C.; Fernandez, V. M. *Biochim. Biophys. Acta* **1987**, *912*, 98–109.

[†] Northwestern University.

[‡] Universidade Nova de Lisboa.

[§] Emory University.

[⊥] University of Georgia.